**46th Annual Review of Progress
in Quantitative Nondestructive Evaluation
QNDE2019
July 14-19, 2019, Portland, OR, USA**

QNDE2019-1234

CONVOLUTIONAL NEURAL NETWORK FOR AUTOMATED DIAGNOSTIC FROM GUIDED WAVE IMAGING IN A STRUCTURAL HEALTH MONITORING CONTEXT

Andrii KULAKOVSKYI[1,2], Roberto MIORELLI[1], Olivier MESNIL[1], Bastien CHAPUIS[1] and Oscar D'ALMEIDA[2]
[1]CEA LIST, Gif-Sur-Yvette, France
[2]SAFRAN, Magny les Hameaux, France

ABSTRACT

This paper presents a Convolutional Neural Network (CNN) based strategy targeting regression and classification tasks based on post-processed Guided Wave Imaging (GWI) images issued from a Structural Health Monitoring (SHM) configuration. The studied use-case is a network of piezo-electric sensors permanently integrated on a structure to inspect. A GWI process is applied to the propagated guided wavepackets between every pair of sensor to generate a picture representing the health of the inspected region. If such image provides to an trained operator both detection and localization by a quick look, automated detection and diagnosis is a challenge, especially if the collected data are noisy. Moreover, GWI does not directly provide information regarding the defect size.

The paper presents the use of a CNN to automate the detection, localization and sizing of a defect. More specifically, to train the CNN, data are generated using a numerical finite element solver, then the theoretical performances of the process are quantified on numerical data. Finally, the model built by the CNN is used to conduct the inversion on real experimental data and excellent detection, localization and sizing are obtained.

Keywords: Structural Health Monitoring, Guided Wave Imaging, Machine Learning, Convolutional Neural Network, Classification, Regression

1. INTRODUCTION

Structural Health Monitoring (SHM) relies on the permanent integration of sensor to detect and quantify flaw. Once the sensors are integrated, this paradigm leads to a much easier inspection process in SHM compared to Non Destructive Testing, especially for recurrent and frequent inspections. However due to the volume of generated data, the diagnostic step must also be automated to provide a relevant information to an operator if an only if a defect of interest has been detected.

One of the most promising approach in SHM is to use Guided Waves (GW), propagating over long distances and highly sensitive to all type of defects and more specifically Guided Wave Imaging. GWI relies on a sparse network of transducers integrated on the structure to generate a picture representing its health. Typically, GW are measured between every pair of transducer, assuming that the defect presence will somehow interfere with the wave packets. The information from every pair of sensor can then be combined using GWI, for example with triangulation-type algorithm such as Delay and Sum (DAS) [1].

The main output of GWI being an image, it is natural to attempt to use tools specifically design to process images, to conduct the automated diagnostic. Toward this end, deep learning algorithms [2] and more specifically Convolutional Neural Network (CNN) [3] can be employed to carry out these tasks. CNN is a recent and major breakthrough in machine learning and allow advanced data classification and regression. It relies on the successive application of filters looking for specific patterns in the image, to update a prediction model. CNN require an extensive database to build an appropriate model.

The use of CNN is enabled by the availability of reliable and efficient numerical simulation tools that can address a large set of realistic problems. The training base for the CNN is generated using the Spectral Finite Element (SFE) described in [4] for a set of predefined parameters. The configuration studied in this paper is a flat aluminum panel with a through-circular hole instrumented by eight piezoelectric transducers located in a circle around an area to monitor. The inspection is conducted by short bursts at 40 kHz and imaging is conducted with the DAS algorithm [1]. The varying parameters are the diameter of the hole along with its size.

The automated diagnostic is first validated with numerical data (similar but not included in the training set) and validated experimentally through an experiment.

2. DATABASE CREATION

The GWI database generation is performed by employing a time domain SFE method [4] of the CIVA software. The main characteristic of the employed SFE method consists first in employing higher-order finite element aiming at reducing the number of elements and secondly in using a macro element pre-meshing procedure adapted to the topology of the targeted problem (e.g., flaw, shape, specimen geometry and characteristics, etc.). The main advantages of SFE method consist in reducing the RAM memory footprint of the simulation and CPU time.

The studied configuration is the imaging of a flat aluminum panel instrumented by eight piezoelectric transducers located in a circle around an area to monitor. The defect is a through-circular hole. For each GW emission, one simulation must be computed for every emitter; therefore, eight simulations must be conducted to obtain a GWI image. At 40 kHz, the complete simulation and processing time is of the order of 5 minutes on a regular desktop computer. A total of 918 images are generated for various flaw positions and sizes. Figure 1 is an example of one of the image included in the dataset.

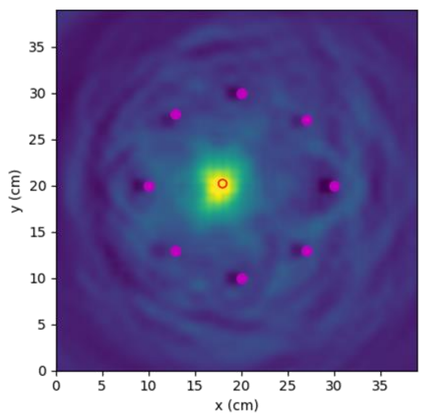

FIGURE 1: EXAMPLE OF DAS BASED POST PROCESSED SIGNALS. THE PINK CIRCLES REPRESENT THE TRANSDUCERS AND THE RED CIRCLE A 10 MM DIAMETER DEFECT. THE COLOR MAP REPRESENT THE RESULT OF THE DAS IMAGING.

3. AUTOMATED DIAGNOSTIC USING CNN

This section explains the deep learning strategy adopted in this paper. In this section, we first define the parametric model adopted then we provide an overview of the learning schema based on CNN employed.

3.1 Description of the parametric model

For sake of generality, let us define a parametric regression problem, involving the generation of a training set composed by a set of E examples of inputs $\mathbf{I}=[\mathbf{i_1},\dots,\mathbf{i_E}]^T$ where the i-th the vector $\mathbf{i_i} \in \mathrm{R}^{Mx \times My \times 1}$ and the targets $\mathbf{T}=[\mathbf{t_1},\dots,\mathbf{t_E}]^T$ where the i-th the vector $\mathbf{t_i} \in \mathrm{R}^{P \times 1}$ where $Mx \times My$ and P represent the dimension of space of inputs and targets, respectively. Therefore, we define the training dataset as the ensemble of ordered couples

$$\mathbf{D}_{\mathrm{trn}} = \{(\mathbf{i}_1, \mathbf{t}_1), \dots, (\mathbf{i}_E, \mathbf{t}_E)\}. \tag{2}$$

In view of classification and regression tasks, the matrix $\mathbf{I}$ represents the E examples and the dimension $Mx \times My$ is associated to the number of pixel (i.e., the measurement points) of the post-processed GW signal. Conversely, the targets matrix $\mathbf{T}$ consists in E rows and P columns representing the size and the position of the different flaws considered. In this work, the training set D_{trn} has been generated via the CIVA software [5].

3.2 Deep learning via convolutional neural network

Very recently, CNN has shown to be very effective in a wide range of practical machine learning tasks ranging from text and image classification, object recognition and many others. Loosely speaking, the main feature of CNN consist in the capability to determine relevant features by properly combining inputs images accordingly to the chosen CNN architecture. The CNN are typically composed by multiple cascades of aggregated convolutional layers. For each aggregated convolutional layer, convolution, activation, average pooling and drop out operations are typically performed. Subsequently, aggregated layers are successively stacked and connected together. The convolution is performed by employing the convolutional operators called kernels. For each of the $Mx \times My$ pixels, the kernel outputs will have a high value if the convolution feature is present at the pixel position, otherwise the output is low. The kernel output can be computed as

$$h_{i,j} = \sum_{k=1}^{m} \sum_{l=1}^{m} w_{k,l} x_{i+k-1,j+l-1}, \tag{3}$$

where $h_{i,j}$ is the convolution output, $w_{k,j}$ is the convolution kernel and $x_{i,j}$ stands for the convolution layer input. Convolution operators are followed by the application of an activation function that generally is non-linear in order to describe complex data. In this work, we employed one of the most used and effective activation function for the CNN called Leaky Rectified Linear Unit (L-ReLU). The last operator applied in an aggregated convolutional layer is the pooling, which consists in a subsampling procedure aiming at decreasing the variance and reducing the computational complexity of the activation map. Since we aim to extract smooth features, we adopted the average pooling procedure. In the final version of the paper, more insight on the adopted CNN architecture will be provided.

4. RESULTS

In this paper, CNN has been applied to both classification and regression tasks. In the studied problem, classification is intended as a discrimination task able to automatically determine whether a test image has been obtained from a flawed or flawless specimen. The accuracy of classification tasks has been assessed through Receiving Operation Characteristic (ROC) curves and confusion matrix tools considering a test set containing both flawed and flawless medium. Moreover, a dedicated noise model has been also included in our GW signals simulations to ensure non-trivial classification. This noise model has enabled to study the robustness of the developed approach in case of noisy/corrupted GWI samples. FIGURE 2 illustrates two example of the images contained in the database. The first image is obtained from a simulation in a pristine state while the second is obtained from a simulation in a damaged state. To the naked eye, it is reasonably difficult to sort the image between pristine and flawed. Moreover, it is completely impossible to visually estimate the size of the defect.

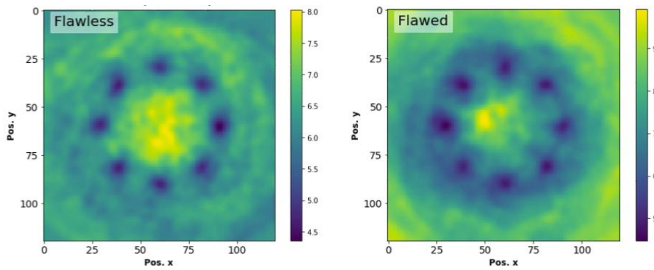

(a) (b)

FIGURE 2: EXAMPLE OF THE IMAGES CONTAINED IN THE LEARNING DATABASE (a): FLAWLESS IMAGE AND (b): FLAWED IMAGE

In FIGURE 3, the classification results based on CNN are provided. The classification was obtained by applying the classifier to 78 pristine images and 72 images containing damages. An excellent success rate is observed. To go further, the ROC curve is also displayed in FIGURE 3.

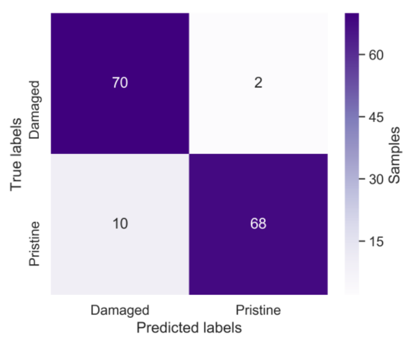

a)

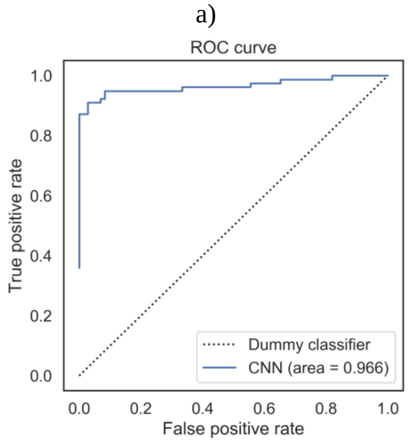

b)

FIGURE 3: CLASSIFICATION RESULT ASSOCIATED TO THE FLAW DETACTION PROBLEM IN a) ARE SHOWED IN TERMS OF CONFUSION MATRIX AND IN b) IN TERMS OF ROC CURVE.

In FIGURE 4, we show the preliminary results obtained by applying CNN in view of regression tasks aiming at retrieving the flaw radius. The red dots represent the inversion of defect size on the same test data as FIGURE 3. The green triangle represent the inversion of the defect size of experimental data acquire on the same configuration.

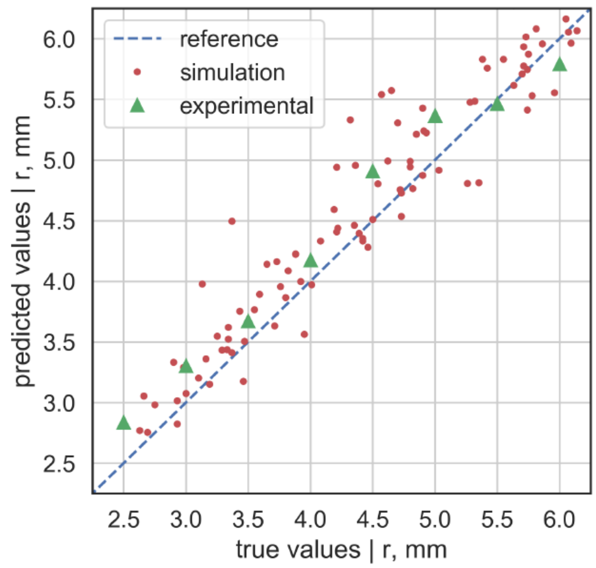

FIGURE 4: REGRESSION RESULT ASSOCIATED TO THE FLAW RADIUS ESTIMATION.

5. CONCLUSION

This work presented a deep learning framework for the automation of the classification and regression tasks based on GWI images. Both the classification and regression are successful on numerical data not included on the training set. The inversion model is also used to invert defect size from experimental data with success.

REFERENCES

[1]: Michaels, J. E., Detection, localization and characterization of damage in plates with an in situ array of spatially distributed ultrasonic sensors, Smart Materials and Structures, IOP Publishing, 2008, 17, 035035.

[2] Goodfellow, L., Bengio, Y., and Courville, A., *Deep Learning*. MIT Press, 2016.

[3] Shang, W., Sohn, K., Almenia, D., and Lee, H.. Understanding and Improving Convolutional Neural Networks via Concatenated Rectified Linear Units, International Conference on Machine Learning. 2016, pp. 2217–2225.

[4] Mesnil, O.; Imperiale, A.; Demaldent, E. & Chapuis, B. Validation of Spectral Finite Element Simulation Tools dedicated to Guided Wave Based Structure Health Monitoring AIP Conference Proceedings, 2019.

[5] http://www.extende.com

